BIOCHEMISTRY
including biophysical chemistry & molecular biology

Article

pubs.acs.org/biochemistry

Lobe-Specific Calmodulin Binding to Different Ryanodine Receptor Isoforms

Kelvin Lau, Mandy M. Y. Chan, and Filip Van Petegem*

Department of Biochemistry and Molecular Biology, Life Sciences Institute, University of British Columbia, Vancouver, British Columbia V6T 1Z3, Canada

Supporting Information

ABSTRACT: Ryanodine receptors (RyRs) are large ion channels that are responsible for the release of Ca^{2+} from the sarcoplasmic/endoplasmic reticulum. Calmodulin (CaM) is a Ca^{2+} binding protein that can affect the channel open probability at both high and low Ca^{2+} concentrations, shifting the Ca^{2+} dependencies of channel opening in an isoform-specific manner. Here we analyze the binding of CaM and its individual domains to three different RyR regions using isothermal titration calorimetry. We compared binding to skeletal muscle (RyR1) and cardiac (RyR2) isoforms, under both Ca^{2+}-loaded and Ca^{2+}-free conditions. CaM can bind all three regions in both isoforms, but the binding modes differ appreciably in two segments. The results highlight a Ca^{2+}/CaM and apoCaM binding site in the C-terminal fifth of the channel. This binding site is the target for malignant hyperthermia and central core disease mutations in RyR1, which affect the energetics and mode of CaM binding.

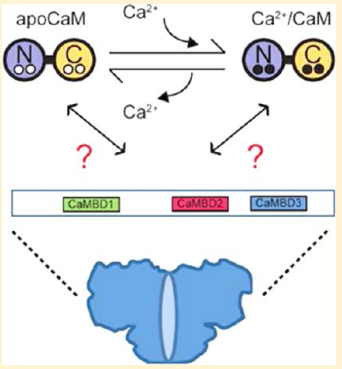

Ryanodine receptors (RyRs) are large ion channels that mediate the release of Ca^{2+} from the endoplasmic/sarcoplasmic reticulum (ER/SR).[1] They are involved in many physiological events that depend on Ca^{2+} as a second messenger, including excitation−contraction (EC) coupling in various types of muscles. In mammalian organisms, three different isoforms have been identified (RyR1−3),[2−4] sharing both sequence and structural homology. All isoforms are expressed in multiple cell types; however, RyR1 is mainly found in skeletal muscle, and RyR2 is abundant in cardiac myocytes.

The primary ligand for triggering RyR opening is cytosolic Ca^{2+}. Under these circumstances, the RyR acts as a signal amplifier, in a process known as Ca^{2+}-induced Ca^{2+} release (CICR).[5,6] However, as Ca^{2+} levels in the cytosol increase, RyRs close, indicating that there are multiple Ca^{2+} binding sites with different affinities and binding kinetics. A plot of the open probability of the channel as a function of Ca^{2+} concentration therefore displays a bell-shaped curve.[7] In addition, luminal Ca^{2+} levels can regulate RyR opening through the process of store overload-induced calcium release (SOICR).[8,9]

The exact timing of channel opening and closing is crucial. Several genetic diseases result from altered RyR activity, often increasing their sensitivity to cytosolic or luminal Ca^{2+} and leading to channels with enhanced open probabilities. RyR1 mutations are mostly associated with malignant hyperthermia (MH)[10] and central core disease (CCD),[11] whereas RyR2 mutations can cause catecholaminergic polymorphic ventricular tachycardia (CPVT).[12] These mutations are found throughout the RyR genes, but many have been found to cluster at domain−domain interfaces.[13−20] Multiple auxiliary proteins can fine-tune the sensitivity of RyRs to Ca^{2+}. A major player is calmodulin (CaM), a 17 kDa protein with four EF hands that can bind Ca^{2+}. CaM directly binds to RyRs, but the effect is dependent on Ca^{2+} concentration and the exact RyR isoform. At high Ca^{2+} levels, CaM can inhibit both RyR1 and RyR2. At low Ca^{2+} levels, it activates RyR1 but inhibits RyR2,[21−24] although the inhibition at low Ca^{2+} concentrations has been controversial.[25] Recent experiments using RyR2 have shown that mutations of the N-lobe of CaM increase the threshold for termination of Ca^{2+} release, whereas mutations of the C-lobe decrease the threshold,[26] suggesting individual roles and possibly distinct binding sites for the lobes on the full-length channel. Interestingly, mutations in CaM have also been associated with CPVT,[27] indicating that a proper regulation of RyR2 by CaM is absolutely required.

How exactly CaM exerts its stimulatory or inhibitory effects is currently unknown. Previously, a number of RyR peptides have been thought to bind CaM based mainly on pull-downs, overlay assays, gel shifts, and fluorescence measurements.[28−36] However, most of these have not been validated using a quantitative method, and multiple ones have been discarded because they have been shown to be inaccessible[15] or do not agree with cryo-electron microscopy (cryo-EM) data, as recently discussed by Huang et al.[37] Thus far, only three RyR segments remain as candidates to be "true" CaM binding sites. CaM has often been shown to use its individual lobes to bridge different peptide stretches in its target proteins, so it is likely that more than one of these segments is involved in binding either Ca^{2+}/CaM or apoCaM.

Received: November 6, 2013
Revised: January 4, 2014
Published: January 21, 2014

dx.doi.org/10.1021/bi401502x | *Biochemistry* 2014, 53, 932−946

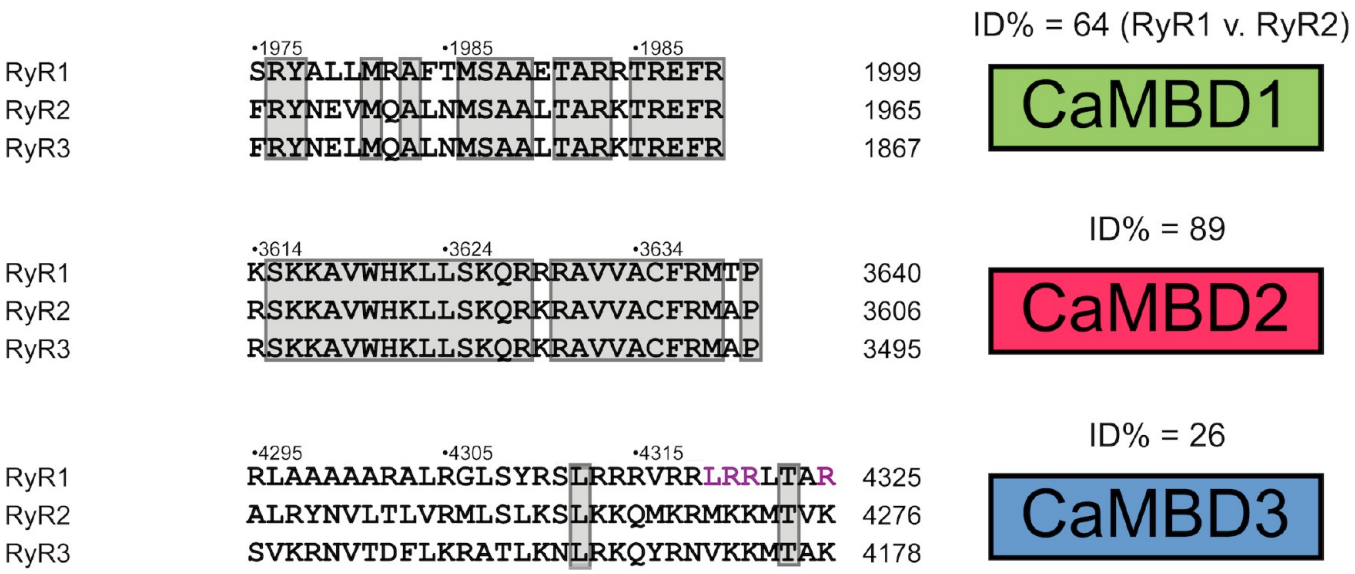

Figure 1. Sequences of three CaM binding domains (CaMBDs). Residues that are strictly conserved among RyR1−RyR3 are highlighted in gray. Purple residues are the sites of mutation in RyR1CBD3, duplication of L4319−4321 and R4325D. The numbering is for rabbit RyR1, mouse RyR2, and human RyR3.

A crystal structure has shown that Ca^{2+}/CaM is able to bind to a peptide in the central region of RyR1 (amino acids 3614−3643), with both CaM lobes binding the segment simultaneously.[38] However, NMR data have shown that the Ca^{2+}/N-lobe is only loosely associated with the peptide, suggesting it is likely to bind elsewhere in full-length channels.[38] Cryo-EM studies have shown that only one CaM binds per RyR monomer,[39] although this does not exclude the possibility that additional CaMs may bind to separate, low-affinity sites. The cryo-EM studies also show that the binding site for CaM on RyR1 shifts by ∼30 Å.[39,40] This shift is too large to be attributed to a different mode of binding to the same peptide and suggests that one or both CaM lobes shift to another sequence stretch upon binding Ca^{2+}. Curiously, these cryo-EM studies have also shown that the apoCaM binding site in RyR2 coincides with the Ca^{2+}/CaM binding site in RyR1. Together with the different functional effects of CaM in the two isoforms, this indicates that the mode of binding in the two isoforms is different.

Because of the complexities by which CaM can bind its targets, and the inherent ability of the individual lobes to bridge different sequence stretches in other proteins, we used isothermal titration calorimetry (ITC) to analyze the binding of CaM and its individual lobes under both apo and Ca^{2+}-loaded conditions. We focused on the three remaining CaM binding candidates [CaM binding domains 1−3 (CaMBD1−CaMBD3, respectively) (Figure 1)] in both RyR1 and RyR2. The data show isoform-specific differences and suggest that the highest affinity for apoCaM resides in the C-terminal region of the RyR. The latter is also the target for disease mutations that affect CaM binding.

EXPERIMENTAL PROCEDURES

Cloning and Purification. Sequences encompassing rabbit RyR1 (CaMBD1, residues 1975−1999; CaMBD2, residues 3614−3640) and rat RyR2 (CaMBD1, residues 1941−1965; CaMBD2, residues 3580−3606; CaMBD3, residues 4246−4276) were cloned in a pET24a vector containing a C-terminal hexahistidine tag using NdeI and XhoI cut sites. At the N-terminus, maltose binding protein (MBP) was attached, along with a cleavage site for tobacco etch virus (TEV) protease. The presence of affinity tags on both sides allows us to extract only peptides without degradation within the CaMBD sequence. RyR1 CaMBD3 (residues 4295−4325) could not be cloned using routine polymerase chain reaction, and instead, synthetic peptides (Lifetein) were used for wild-type and disease mutant versions. To protect the fusion proteins from proteolytic degradation, they were co-expressed with human CaM, which binds and prevents access to proteases. The CaM was co-expressed in a peGST vector,[41] using *Escherichia coli* Rosetta-(DE3) pLacI at 37 °C and induced at an OD_{600} of ∼0.6 by addition of 0.2 mM IPTG for 4 h. Cells were lysed by sonication in buffer A [250 mM KCl, 10 mM $CaCl_2$, and 10 mM HEPES (pH 7.4)] supplemented with 25 mg mL^{-1} DNase I, 25 mg mL^{-1} lysozyme, 1 mM iodoacetamide, and 1 mM phenylmethanesulfonyl fluoride. The lysate was applied to a 25 mL Poros MC column (Tosoh Bioscience), washed with 5 column volumes (CV) of buffer A and 5 CV of 2% (v/v) buffer B [250 mM KCl, 10 mM $CaCl_2$, and 500 mM imidazole (pH 7.4)], and eluted with 30% (v/v) buffer B. The protein was diluted 2-fold with buffer A and then applied to a 25 mL amylose column (New England Biolabs). The protein was then washed with 20 CV of buffer A and 10 mM EDTA and 2 CV of buffer A and eluted with buffer C (buffer A with 10 mM maltose). The wash step with EDTA completely removed the co-expressed CaM. The protein was diluted 2-fold with buffer A and applied once again to a 25 mL Poros MC column, washed, and eluted as described above. For the CaMBD2 constructs, which contain cysteines, 10 mM β-mercaptoethanol (BME) was present in all buffers except for those used for the Poros MC column. The fusion proteins were confirmed to be monomeric using size exclusion chromatography on a Superdex200 column (GE Healthcare) (Figure 1 of the Supporting Information). The molecular weights were confirmed by matrix-assisted laser desorption ionization time-of-flight (MALDI-TOF) on a Voyager-DE STR instrument (Applied Biosystems) as fusion proteins and as peptides after cleavage with TEV protease.

Cloning and Purification of Calmodulin and Its Lobes. Full-length human CaM, its N-terminal lobe (N-lobe, residues 1−78), and its C-terminal lobe (C-lobe, residues 79−149) were

dx.doi.org/10.1021/bi401502x | *Biochemistry* 2014, 53, 932−946

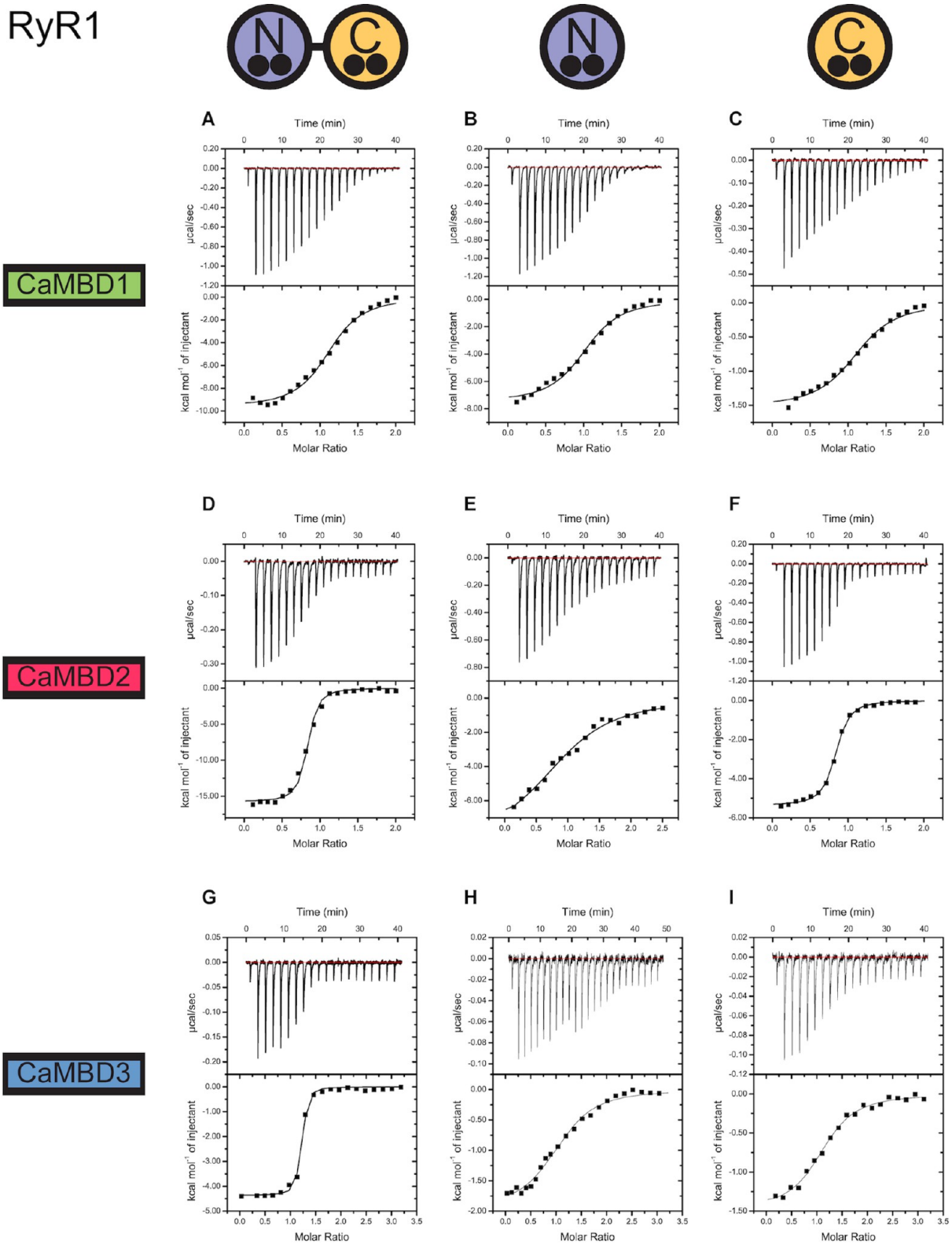

Figure 2. Ca^{2+}/CaM and its lobes bind to all three RyR1 CaMBDs. (A–I) ITC binding isotherms show the interaction between CaM or its lobes titrated into each CaMBD in the presence of 10 mM $CaCl_2$. The columns indicate the titrant; the rows show the CaMBD in the cell. Solid lines represent the fits. The following concentrations were used (titrant into cell): (A) 500 μM in 50 μM, (B) 1330 μM in 133 μM, (C) 1330 μM in 133 μM, (D) 150 μM in 15 μM, (E) 1000 μM in 80 μM, (F) 800 μM in 80 μM, (G) 223 μM in 22.3 μM, (H) 490.9 μM in 31.5 μM, and (I) 315 μM in 31.5 μM. Affinity and thermodynamic parameters are listed in Table 1.

cloned as described previously[42] into a modified pET28 vector containing an N-terminal hexahistidine tag and a tobacco etch virus (TEV) protease cleavage site. Purification was like that for the CaMBD constructs, with the following exception. After the first Poros MC column, the protein was cleaved with His-tagged TEV protease overnight at room temperature while being

dx.doi.org/10.1021/bi401502x | *Biochemistry* 2014, 53, 932–946

Table 1. Thermodynamic Parameters of Binding between Ca^{2+}/CaM and Its Lobes and CaMBDs in 10 mM $CaCl_2$[a]

	construct	lobe	no. of sites (N)	K_d (μM)	ΔH (kcal/mol)	ΔS (cal mol^{-1} deg^{-1})	n
RYR1							
	CaMBD1	CaM	0.81 ± 0.22	2.05 ± 0.96	−9.36 ± 1.25	−5.21 ± 3.6	4
		N	0.79 ± 0.33	5.95 ± 2.07	−8.81 ± 1.82	−5.58 ± 5.4	2
		C	0.88 ± 0.35	7.88 ± 0.74	−1.49 ± 0.04	18.4 ± 0.4	2
	CaMBD2	CaM	0.75 ± 0.14	0.046 ± 0.032	−16.8 ± 2.9	−18.3 ± 6.3	4
		N	0.87 ± 0.11	33.3 ± 10.7	−10.7 ± 2.1	−15.4 ± 7.7	3
		C	0.80 ± 0.03	0.80 ± 0.29	−5.94 ± 0.57	8.09 ± 1.83	4
	CaMBD3	CaM	1.02 ± 0.19	0.052 ± 0.022	−5.00 ± 1.19	16.7 ± 3.5	6
		N	1.07 ± 0.08	4.19 ± 1.44	−4.18 ± 2.27	10.7 ± 8.0	6
		C	1.16 ± 0.27	2.62 ± 1.22	−2.77 ± 1.95	16.5 ± 7.1	6
RYR2							
	CaMBD1	CaM	0.71 ± 0.04	7.59 ± 1.05	−6.09 ± 0.14	3.01 ± 0.76	2
		N	0.75 ± 0.11	26.7 ± 8.7	−5.52 ± 0.74	2.47 ± 2.66	2
		C	binding detected but not quantifiable				4
	CaMBD2	CaM	0.77 ± 0.13	0.047 ± 0.017	−17.2 ± 1.1	−24 ± 2.8	3
		N	1.13 ± 0.28	18.9 ± 7.9	−7.25 ± 0.47	−2.44 ± 4.13	4
		C	1.16 ± 0.41	1.03 ± 0.75	−5.09 ± 0.18	10.6 ± 6.1	3
	CaMBD3	CaM	complex binding				4
		N, K_{d1}	1.06 ± 0.11	0.052 ± 0.015	−1.28 ± 0.16	29.1 ± 0.9	4
		N, K_{d2}	1.14 ± 0.08	4.6 ± 0.4	3.79 ± 0.18	37.2 ± 0.5	4
		C	1.04 ± 0.01	3.09 ± 1.12	1.99 ± 0.18	31.7 ± 0.5	4

[a]Values are averages of n measurements. Errors are standard deviations.

Table 2. Thermodynamic Parameters of Binding between Ca^{2+}/CaM and Its Lobes in Competition Experiments and CaMBDs in 10 mM $CaCl_2$[a]

	construct	lobe	no. of sites (N)	K_d (μM)	ΔH (kcal/mol)	ΔS (cal mol^{-1} deg^{-1})	n
RYR1							
	CaMBD1	N > C	0.71 ± 0.18	22.4 ± 6.8	−6.44 ± 0.17	−0.27 ± 0.05	2
		C > N	heats indistinguishable from background				1
	CaMBD2	N > C	0.67 ± 0.05	60.7 ± 27.2	−6.40 ± 1.94	−2.04 ± 7.31	3
		C > N	0.44 ± 0.02	8.00 ± 1.35	−1.08 ± 0.07	19.7	1
RYR2							
	CaMBD3	N > C	0.51 ± 0.20	5.86 ± 4.54	−2.50 ± 0.80	16.0 ± 4.3	3
		C > N	heats indistinguishable from background				1

[a]Values are averages of n measurements. Errors are standard deviations (for n = 1, errors are deviations of the fit from data).

dialyzed against buffer A. The tagged protease and cleavage product were removed with an additional Poros MC column. The flow-through was applied to a Phenyl-Sepharose HP column (GE Healthcare) equilibrated with 150 mM KCl, 20 mM HEPES (pH 7.4), and 10 mM $CaCl_2$. The protein was eluted with the same buffer containing 10 mM EDTA instead of $CaCl_2$, applied to a HiLoad Q-Sepharose HP column equilibrated with 20 mM HEPES (pH 7.4) and 10 mM EDTA, and eluted with a gradient from 20 to 40% buffer containing an additional 1 M KCl over 14 CV. Molecular weights for all proteins were confirmed by MALDI-TOF on a Voyager-DE STR instrument (Applied Biosystems).

ITC. The purified MBP−CaMBD fusion proteins were dialyzed against 150 mM KCl, 10 mM HEPES (pH 7.4), 10 mM 2-mercaptoethanol, 10 mM $CaCl_2$, or 10 mM EDTA at 4 °C. Peptides that were synthesized and delivered as lyophilized powder (Lifetein) were dissolved directly in dialysis buffer. The peptide oligomeric state was confirmed to be monomeric on a Superdex75 column (GE Healthcare) (Figure 1 of the Supporting Information). Concentrations were determined using the calculated extinction coefficient at 280 nm in the presence of 6 M guanidine.[43] Titrations consisted of 20 injections of 2 μL of titrant (CaM or lobes) into the cell containing a CaMBD at a 10-fold lower concentration. Typical concentrations for the titrant were between 100 and 500 μM for experiments in 10 mM $CaCl_2$ and between 700 and 2000 μM for experiments in 10 mM EDTA, depending on the affinity. Experiments were performed at 25 °C and a stirring speed of 1000 rpm on an ITC200 instrument (GE Healthcare). Control experiments titrating CaM or its lobes (2000 μM) into the hexahistidine-tagged MBP without CaMBD2 (200 μM) in 10 mM $CaCl_2$ or 10 mM EDTA showed heats that were indistinguishable from buffer injections (data not shown). In addition, control experiments titrating the N-lobe (2000 μM) into the C-lobe (200 μM) in the presence of 10 mM $CaCl_2$ or 10 mM EDTA show heats that are indistinguishable from buffer injections (data not shown). The data were processed using Origin 7.0 and fit to a one- or two-site fitting model after background buffer subtraction.

RESULTS

Binding to CaMBD2. A previously published crystal structure reported a complex between Ca^{2+}/CaM and a peptide in the central region of RyR1 (amino acids 3614−3643).[38] We termed this CaMBD2 simply to reflect its position in the sequence relative to other CaM binding domains investigated in this study (Figure 1). We utilized ITC to explore the

dx.doi.org/10.1021/bi401502x | Biochemistry 2014, 53, 932−946

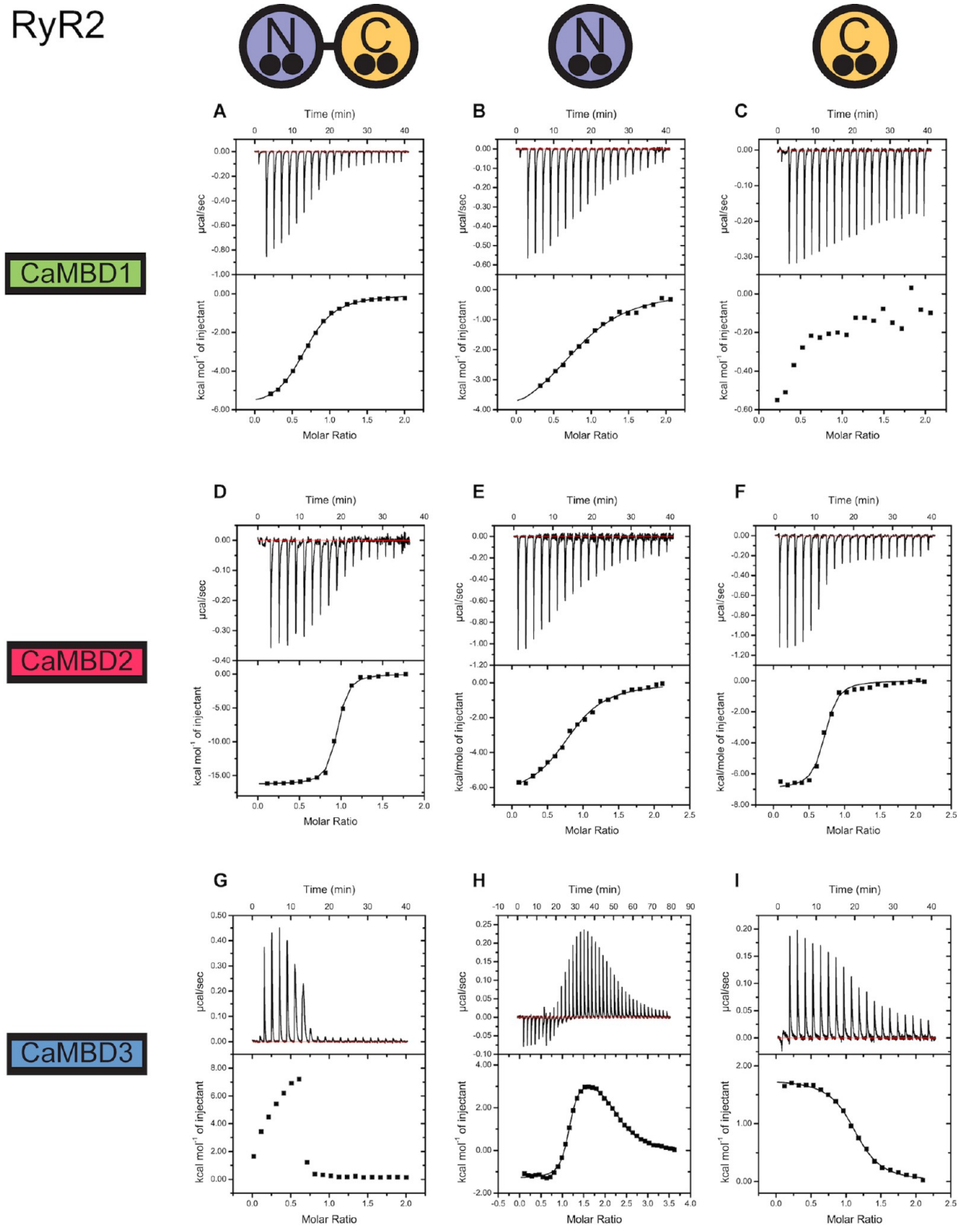

Figure 3. Ca^{2+}/CaM and its lobes bind to all three RyR2 CaMBDs. (A–I) ITC binding isotherms show the interaction between CaM or its lobes titrated into each CaMBD in the presence of 10 mM $CaCl_2$. The columns indicate the titrant; the rows show the CaMBD in the cell. Solid lines represent the fits. The following concentrations were used (titrant into cell): (A) 1100 μM in 110 μM, (B) 1132 μM in 110 μM, (C) 1132 μM in 110 μM, (D) 150 μM in 15 μM, (E) 788 μM in 79 μM, (F) 674 μM in 67 μM, (G) 630 μM in 63 μM, (H) 1109 μM in 63 μM, and (I) 661 μM in 63 μM. Affinity and thermodynamic parameters are listed in Table 1. The binding isotherm in panel C could not be accurately fit because of the low affinity.

thermodynamic parameters that underlie the binding. Because physiological concentrations of Ca^{2+} would yield mixtures of Ca^{2+}-free and Ca^{2+}-occupied lobes, the experiments were performed in the presence of excess Ca^{2+} (10 mM) to saturate all Ca^{2+} binding sites and to isolate binding of a fully Ca^{2+}-occupied CaM. The interaction of Ca^{2+}/CaM is strong, with a K_d

dx.doi.org/10.1021/bi401502x | *Biochemistry* 2014, 53, 932–946

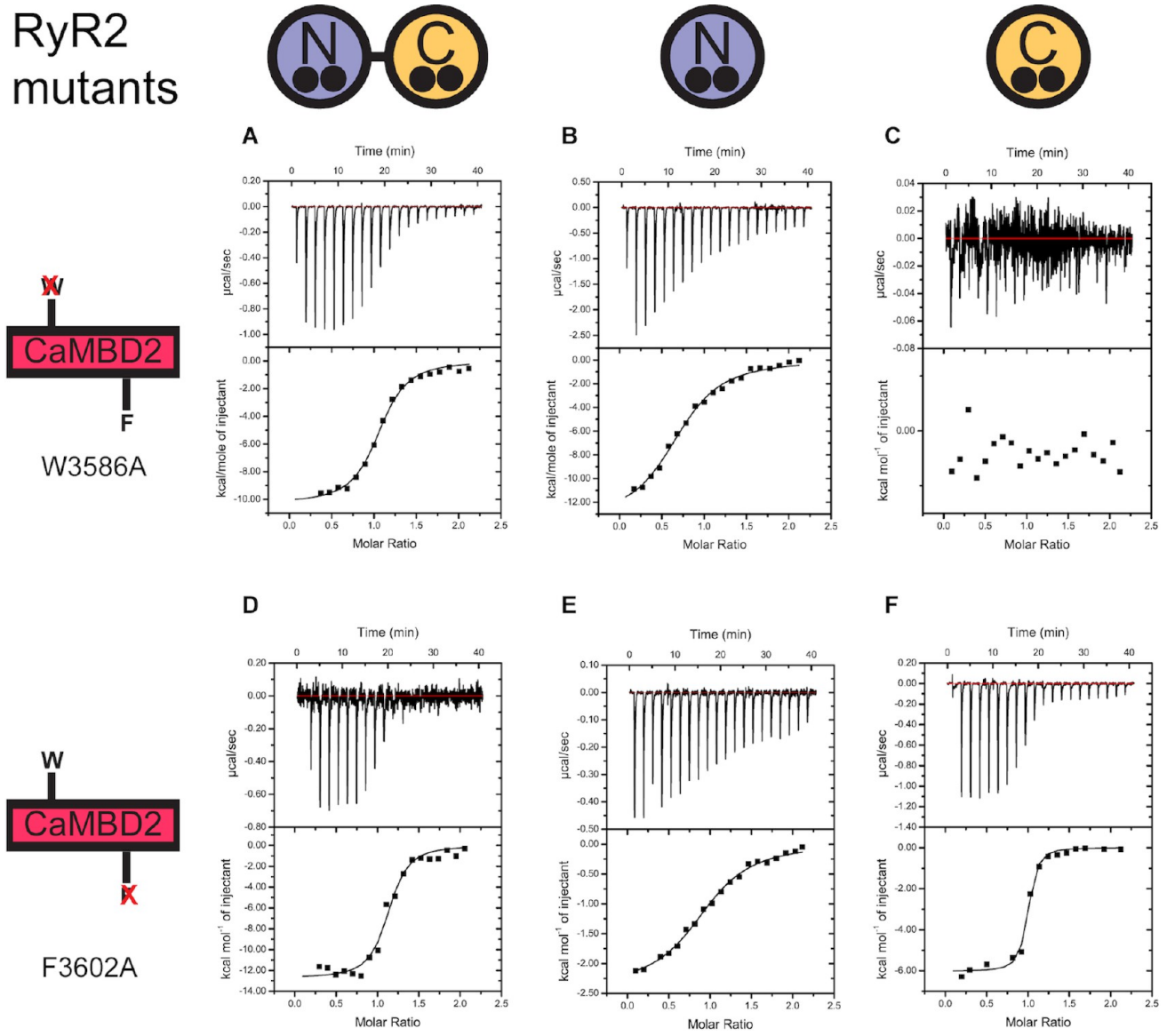

Figure 4. RyR2 CaMBD2 W3586A and F3602A mutants alter lobe binding. (A–F) ITC binding isotherms show the interaction between CaM or its lobes titrated into each mutant CaMBD in the presence of 10 mM $CaCl_2$. The columns indicate the titrant; the rows show the CaMBD in the cell. Solid lines represent the fits. The following concentrations were used (titrant into cell): (A) 500 μM in 50 μM, (B) 1000 μM in 100 μM, (C) 521 μM in 52 μM, (D) 500 μM in 50 μM, (E) 788 μM in 79 μM, and (F) 674 μM in 67 μM. Affinity and thermodynamic parameters are listed in Table 3.

of 46 nM (Figure 2 and Table 1). The binding is driven by enthalpy and has an unfavorable entropic contribution. To determine the contribution of each CaM lobe, we also investigated their binding individually. Ca^{2+}/C-lobe binds much stronger ($K_d \sim 800$ nM) than the Ca^{2+}/N-lobe ($K_d \sim 33$ μM). The Ca^{2+}/C-lobe is driven by favorable entropy and enthalpy, while Ca^{2+}/N-lobe binding is driven by enthalpy alone.

As it is possible that both lobes compete for an overlapping binding site, we performed competition experiments with the Ca^{2+}/C-lobe premixed with RyR1 CaMBD2 (Figure 2 of the Supporting Information and Table 2). These show that the affinity of CaMBD2 for the Ca^{2+}/N-lobe, once the Ca^{2+}/C-lobe has been bound, is even lower ($K_d \sim 60$ μM). The ability of the weaker Ca^{2+}/N-lobe to still bind in the presence of excess Ca^{2+}/C-lobe indicates that the binding sites are not mutually exclusive, but the weaker apparent affinity shows there is some additional strain when both lobes bind.

As Ca^{2+}/CaM has different effects on RyR1 and RyR2, we wondered whether there are any differences in the binding affinities or energetic signatures of either lobe between both isoforms. However, the corresponding peptide in RyR2 binds with a very similar affinity, enthalpy, and entropy, and as for RyR1, the Ca^{2+}/C-lobe forms the major interaction (Figure 3 and Table 1). Thus, in agreement with the large amount of sequence conservation among the different RyR isoforms, the overall binding mode on CaMBD2 is likely to be very similar.

In the crystal structure of the RyR1–CaMBD2 complex,[38] a Trp residue forms the main anchor point for the Ca^{2+}/C-lobe whereas a Phe residue provides the major contacts with the Ca^{2+}/N-lobe. We used individual lobes with mutant CaMBD2s to further dissect this interaction. In agreement with this, the W3586A mutation in RyR2 completely abolishes binding of the Ca^{2+}/C-lobe to CaMBD2, while the F3602A mutation has no effect (Figure 4 and Table 3). However, both W3586A and F3602A still allow for Ca^{2+}/N-lobe binding, but with different

dx.doi.org/10.1021/bi401502x | *Biochemistry* 2014, 53, 932–946

Table 3. Thermodynamic Parameters of Binding between Ca^{2+}/CaM and Its Lobes and Mutant CaMBDs in 10 mM $CaCl_2$[a]

construct	lobe	no. of sites (N)	K_d (μM)	ΔH (kcal/mol)	ΔS (cal mol^{-1} deg^{-1})	n
RYR2						
CaMBD2W3586A	CaM	0.91 ± 0.16	1.01 ± 0.43	−11.9 ± 2.6	−12.3 ± 9.3	4
	N	0.69 ± 0.39	18.9 ± 7.6	−12.8 ± 0.7	−21.3 ± 2.0	3
	C		heats indistinguishable from background			4
CaMBD2F3602A	CaM	1.10 ± 0.02	0.32 ± 0.09	−12.7 ± 0.4	−13.0	1
	N	0.96 ± 0.02	6.86 ± 1.43	−1.86 ± 0.02	17.4 ± 1.8	2
	C	0.78 ± 0.50	0.44 ± 0.29	−7.66 ± 0.09	3.8 ± 3.6	3
RYR1						
CaMBD3LRRdup	CaM	0.79 ± 0.14	0.014 ± 0.008	−10.3 ± 1.4	1.6 ± 3.9	3
	N	0.82 ± 0.05	2.35 ± 0.67	−7.37 ± 0.31	1.1 ± 1.6	2
	C	0.88 ± 0.25	1.21 ± 0.16	−8.21 ± 2.18	−0.5 ± 7	3
CaMBD3R4325D	CaM	0.64 ± 0.02	0.12 ± 0.005	−9.03 ± 0.06	1.4 ± 0.2	3
	N	0.83 ± 0.03	5.11 ± 0.46	−6.35 ± 0.17	2.9 ± 0.7	3
	C	1.01 ± 0.09	1.54 ± 0.11	−6.04 ± 0.03	6.4 ± 0.12	3

[a]Values are averages of n measurements. Errors are standard deviations (for n = 1, errors are deviations of the fit from data).

affinities and enthalpic components, suggesting that the Ca^{2+}/N-lobe can bind to two different sites. When one Ca^{2+}/N-lobe site is abolished, it can still bind another, a type of behavior that has been observed in other CaM targets.[42,44,45] These data are in agreement with previous studies showing that neither the equivalent W3586A nor the F3602A mutation individually can knock out Ca^{2+}/CaM binding in full-length RyR2.[32] Overall, these data suggest that CaMBD2 primarily forms a high-affinity Ca^{2+}/C-lobe binding site, whereas the binding site for the Ca^{2+}/N-lobe, as observed in the crystal structure, is weak and mobile.

We also analyzed binding of apoCaM to CaMBD2 by repeating the ITC experiments in the absence of Ca^{2+} and in the presence of excess EDTA (Figures 5 and 6 and Table 4). ApoCaM is able to bind CaMBD2 from either isoform, but significantly weaker than Ca^{2+}/CaM (K_d = 50−70 μM). The individual lobes are also capable of binding independently, but the binding was too weak to be quantified reliably. These data show that both apo lobes contribute to the binding of apoCaM to CaMBD2.

Binding to CaMBD1. As the affinity of the Ca^{2+}/N-lobe for CaMBD2 is low, especially in the presence of a prebound Ca^{2+}/C-lobe, we tested the binding to another segment, CaMBD1 (amino acids 1975−1999 in RyR1), which was previously suggested to form a binding site based on gel shift assays.[35] Cross-linking studies also imply that it is close to CaMBD2.[35] This site is less conserved than CaMBD2 between the isoforms (Figure 1), with 64% sequence identity between RyR1 and RyR2. In RyR1, CaMBD1 binds Ca^{2+}/CaM with a K_d of ∼2 μM. Both the Ca^{2+}/N-lobe and Ca^{2+}/C-lobe can bind, but their affinities are weaker than for full-length Ca^{2+}/CaM, indicating that both contribute to the avidity (Figure 2 and Table 1). In the presence of the prebound Ca^{2+}/C-lobe, the affinity of the Ca^{2+}/N-lobe for CaMBD1 is weakened ∼3.5-fold (Figure 2 of the Supporting Information and Table 2), suggesting that the binding of both lobes simultaneously induces some strain.

The CaMBD1 sequences of RyR1 and RyR2 differ in nine positions (Figure 1), and this affects the binding of Ca^{2+}/CaM. In RyR2, Ca^{2+}/CaM binds ∼4-fold weaker, with an affinity of ∼7.6 μM. The Ca^{2+}/N-lobe binds with a K_d of ∼27 μM, but Ca^{2+}/C-lobe titrations yielded a flat binding isotherm that could not be fit reliably, suggesting the interaction is extremely weak (Figure 4 and Table 1). As in RyR1, the affinity of Ca^{2+}/CaM is higher than for either lobe, indicating that both lobes can still contribute to the binding. The main difference between RyR1 and RyR2 thus seems to be a higher affinity for CaMBD1 of RyR1, and only a very small contribution of the Ca^{2+}/C-lobe to RyR2−CaMBD1 binding. Unlike CaMBD2, apoCaM was not observed to bind to CaMBD1 from either isoform (Figures 5 and 6 and Table 4).

In summary, CaMBD1 forms a Ca^{2+}/CaM binding site that is mainly driven by the Ca^{2+}/N-lobe. This lobe binds CaMBD1 stronger than it binds CaMBD2 (when a Ca^{2+}/C-lobe is prebound to it), suggesting that Ca^{2+}/CaM could bridge these two segments.

Binding to CaMBD3. Yet another segment, located in the C-terminal fifth of the channel, has been suggested to form a putative CaM binding site.[28,33] The analyzed segment, termed CaMBD3, spans residues 4295−4325 in RyR1. The sequences of RyR1 and RyR2 are only ∼26% identical in this region (Figure 1).

In RyR1, CaMBD3 forms a high-affinity Ca^{2+}/CaM binding site (K_d ∼ 52 nM) with favorable enthalpy and entropy (Figure 2 and Table 1). The individual lobes bind as well, but with weaker affinities (K_d = 2−4 μM), indicating that both contribute to Ca^{2+}/CaM binding.

The corresponding region in RyR2 interacts with Ca^{2+}/CaM in a completely different manner as it exhibits a complex binding isotherm that cannot be fit using a simple 1:1 binding model (Figure 3 and Table 1). Such complex isotherms have been observed before for CaM−peptide interactions in other ion channels and are likely due to a single CaM binding two peptides in the initial stage of the ITC experiment (when sufficient free peptide is available), followed by unbinding of one peptide and a 1:1 stoichiometry at the later stages (when free peptide is scarce).[42] Despite our inability to fit this isotherm, the sharp transition suggests that the affinity is very high. To deconstruct this complex curve, we also analyzed the binding of the individual CaM lobes. The Ca^{2+}/C-lobe binds with a K_d of ∼3 μM, similar to that of RyR1−CaMBD3 binding. However, the Ca^{2+}/N-lobe titrations show two transitions, revealing a high-affinity site with a K_d of 52 nM driven by both favorable entropy and enthalpy and a second low-affinity site (K_d ∼ 4.6 μM) with unfavorable enthalpy. We used a competition experiment to determine whether both sites are available in the presence of the Ca^{2+}/C-lobe (Figure 2 of the Supporting Information and Table 2). In the presence of the Ca^{2+}/C-lobe, only one exothermic Ca^{2+}/N-lobe binding event was observed with a K_d of 5.9 μM. Overall, the binding mode and energetics of binding of Ca^{2+}/CaM to

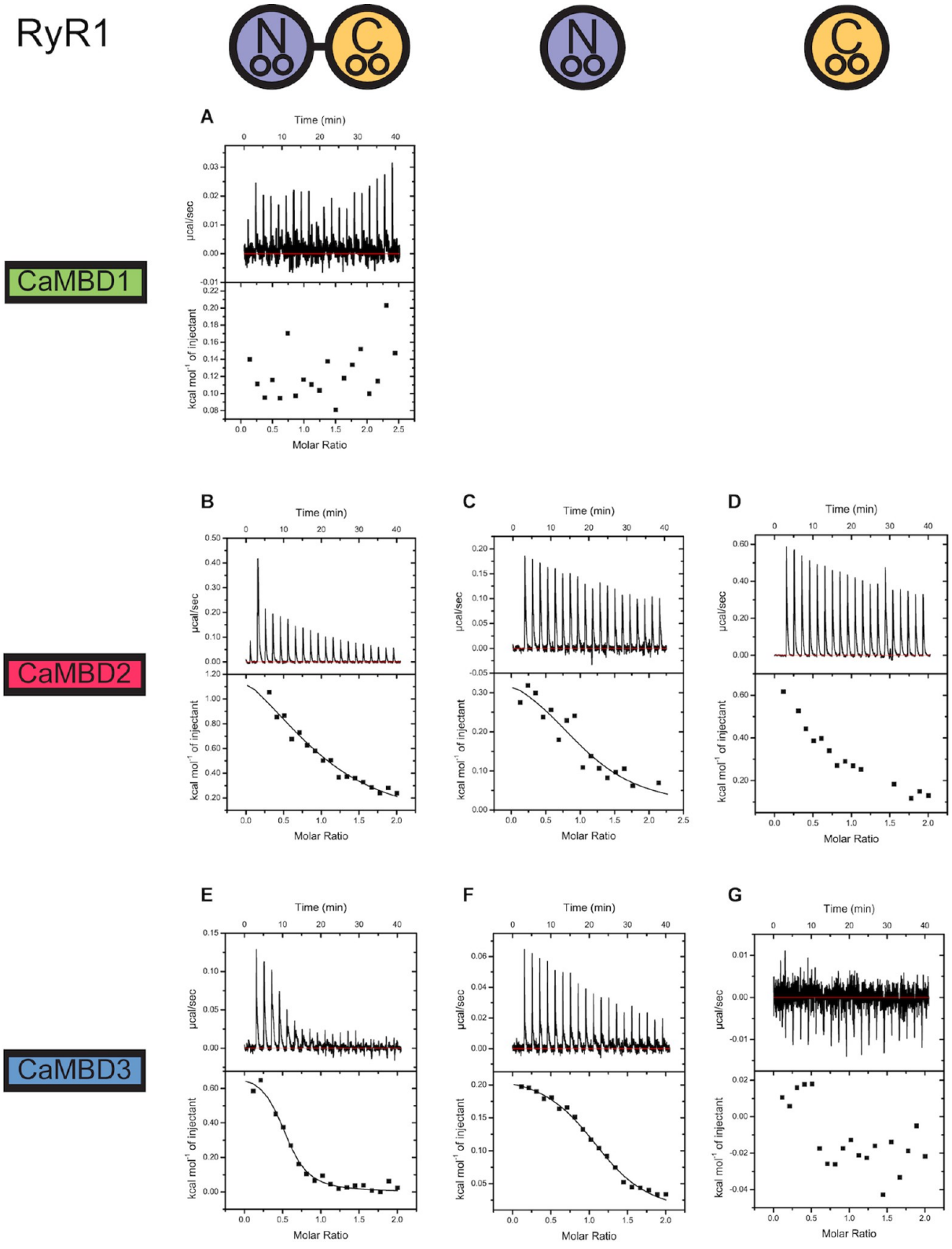

Figure 5. Binding of apoCaM and its lobes to RyR1 CaMBDs. (A–G) ITC binding isotherms show the interaction between CaM or its lobes titrated into each CaMBD in the presence of 10 mM EDTA. The columns indicate the titrant; the rows show the CaMBD in the cell. Solid lines represent the fits. The following concentrations were used (titrant into cell): (A) 1000 μM in 82 μM, (B) 1500 μM in 150 μM, (C) 2264 μM in 200 μM, (D) 1435 μM in 200 μM, (E) 1500 μM in 150 μM, (F) 1500 μM in 150 μM, and (G) 1500 μM in 150 μM. Affinity and thermodynamic parameters are listed in Table 4.

CaMBD3 in both isoforms thus appear to be very different (Figure 7).

Importantly, CaMBD3 also forms a binding site for apoCaM in both RyR1 ($K_d \sim 27$ μM) and RyR2 ($K_d \sim 5$ μM) (Figures 5 and 6 and Table 4). These values show that apoCaM can bind CaMBD3 significantly stronger than CaMBD2, suggesting that CaMBD3 may form the primary binding site for apoCaM. The two isoforms differ appreciably in their apoCaM binding. In

dx.doi.org/10.1021/bi401502x | *Biochemistry* 2014, 53, 932–946

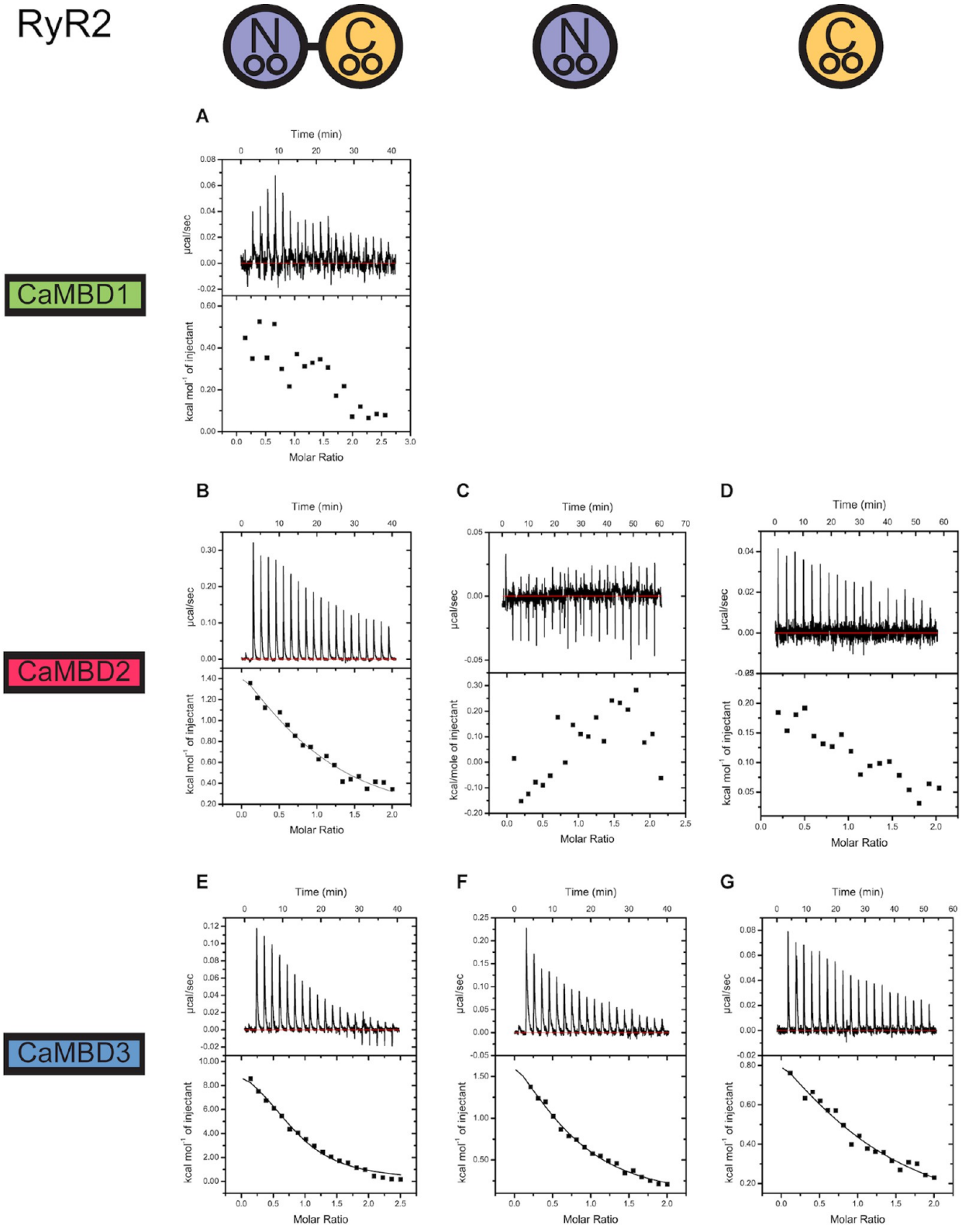

Figure 6. Binding of apoCaM and its lobes to RyR2 CaMBDs. (A–G) ITC binding isotherms show the interaction between CaM or its lobes titrated into each CaMBD in the presence of 10 mM EDTA. The columns indicate the titrant; the rows show the CaMBD in the cell. Solid lines represent the fits. The following concentrations were used (titrant into cell): (A) 760 μM in 60 μM, (B) 1000 μM in 100 μM, (C) 1000 μM in 100 μM, (D) 1000 μM in 100 μM, (E) 250 μM in 25 μM, (F) 750 μM in 75 μM, and (G) 750 μM in 75 μM. Affinity and thermodynamic parameters are listed in Table 4.

RyR1, the binding seems to involve only the apo-N-lobe (K_d ~ 23 μM), whereas in RyR2, both lobes contribute to apoCaM binding (K_d values of ~50 and ~60 μM for the apo-N-lobe and apo-C-lobe, respectively).

In conclusion, CaMBD3 forms the strongest apoCaM binding site of the peptides tested and forms an additional high-affinity site for Ca^{2+}/CaM. Both the sequence and binding mode differ appreciably between both isoforms.

dx.doi.org/10.1021/bi401502x | *Biochemistry* 2014, 53, 932–946

Table 4. Thermodynamic Parameters of Binding between ApoCaM and Its Lobes and CaMBDs in 10 mM EDTA[a]

	construct	lobe	no. of sites (N)	K_d (μM)	ΔH (kcal/mol)	ΔS (cal mol^{-1} deg^{-1})	n
RYR1							
	CaMBD1	apoCaM		heats indistinguishable from background			3
		apo-N-lobe		heats indistinguishable from background			1
		apo-C-lobe		not performed			-
	CaMBD2	apoCaM[b]	1	46.5 ± 22.5	1.59 ± 0.09	26 ± 2	3
		apo-N-lobe	1.09 ± 0.10	55.6 ± 36.4	0.34 ± 0.09	20.8	1
		apo-C-lobe		binding detected but not quantifiable			1
	CaMBD3	apoCaM[c]	0.38 ± 0.09	27.1 ± 14.6	1.5 ± 0.5	26 ± 1	4
		apo-N-lobe	0.90 ± 0.40	22.7 ± 7.7	0.90 ± 0.46	24.3 ± 2.4	3
		apo-C-lobe		heats indistinguishable from background			2
RYR2							
	CaMBD1	apoCaM		heats indistinguishable from background			5
		apo-N-lobe		heats indistinguishable from background			3
		apo-C-lobe		heats indistinguishable from background			2
	CaMBD2	apoCaM	0.89 ± 0.82	72.3 ± 28.6	2.2 ± 2.2	26.3 ± 4.7	2
		apo-N-lobe		heats indistinguishable from background			3
		apo-C-lobe		binding detected but not quantifiable			2
	CaMBD3	apoCaM	0.87 ± 0.26	5.11 ± 2.69	13.2 ± 7.8	68.8 ± 26.7	4
		apo-N-lobe	1.25 ± 0.07	49.3 ± 29.9	2.2 ± 1.7	27.3 ± 2.1	2
		apo-C-lobe	1.01 ± 0.13	62.1 ± 33	1.7 ± 0.2	25.2 ± 1.7	2

[a]Values are averages of n measurements. Errors are standard deviations (for n = 1, errors are deviations of the fit from data). [b]This value was forced to be 1 to allow for fitting. [c]This lower value suggests that one calmodulin binds two peptides (i.e., N = 0.5). This is possible as apo-C-lobe binding is enthalpically silent and undetectable and overlaps with the apo-N-lobe site.

Disease Mutations in RyR1 CaMBD3. Interestingly, two disease mutations map into the CaMBD3 sequence of RyR1 (Figure 1). R4325D has been linked to CCD and multiminicore disease.[46] The second mutation involves a duplication event from L4319 to R4321, which repeats the sequence LRR and has been linked to increased levels of serum creatine kinase and potentially causes MH.[46]

Compared to wild-type CaMBD3, the R4325D mutant weakly affects Ca^{2+}/CaM binding (K_d value of 120 nM vs K_d value of 52 nM) (Figure 8 and Table 3). However, apoCaM binding appears to be stronger (K_d value of ~7 μM vs K_d value of ~27 μM) (Figure 3 of the Supporting Information).

In contrast, the LRR duplication mutant binds Ca^{2+}/CaM ~3.5-fold stronger (14 nM) than the wild type (52 nM), and the affinities of each lobe individually have changed (Figure 8 and Table 3). Under Ca^{2+}-free conditions, the LRR duplication mutant produces a complex binding isotherm with both endothermic and exothermic components (Figure 3 of the Supporting Information). Experiments with the individual lobes show that apo-N-lobe binding is endothermic whereas apo-C-lobe binding is exothermic. This is different from the case for WT CaMBD3, which shows a single endothermic binding event and where direct apo-C-lobe binding could not be detected.

In conclusion, both disease mutations have direct effects on the binding of both apoCaM and Ca^{2+}/CaM to RyR1 CaMBD3.

DISCUSSION

CaM has been identified as a resident Ca^{2+} sensor for multiple ion channel families, including voltage-gated calcium and sodium channels, small conductance Ca^{2+}-activated potassium channels, KCNQ potassium channels, and many more.[47−50] In many cases, the primary role of CaM seems to be affecting the gating properties (opening, closing, and inactivation) of these channels, but it has also been involved in channel trafficking.[51−54]

RyRs are sensitive signal amplifiers: increases in cytosolic Ca^{2+} concentrations trigger their opening, through a phenomenon known as Ca^{2+}-dependent Ca^{2+} release. Although the skeletal muscle isoform (RyR1) can be activated through direct mechanical coupling with L-type Ca^{2+} channels,[55−58] they are also gated by Ca^{2+} ions. CaM can fine-tune the precise sensitivity to Ca^{2+} concentrations, in a manner that appears to be isoform-specific. How exactly this happens remains unknown, but cryo-EM images have shown that the cytoplasmic cap of RyRs undergoes large conformational changes during opening and closing.[59,60] Both apoCaM and Ca^{2+}/CaM have been shown to bind to the lateral side of the cap[39] and are likely to interfere with these allosteric motions. For example, by stabilizing the closed state or destabilizing the open state, Ca^{2+}/CaM would exert an inhibition. In both RyR1 and RyR2, Ca^{2+}/CaM seems to inhibit the channel.[21−24]

To understand the mechanisms that underlie CaM regulation of RyRs, it is necessary to know which regions of the RyR sequence can bind CaM and under which conditions. Several RyR regions have been proposed as CaM binding sites,[28−36] but in many cases, these sites were not validated using a quantitative method. In fact, most of the initially identified sites have been shown to be inaccessible within a folded domain[15] or were found to be located too far from the CaM binding site identified in cryo-EM studies.[37] A crystal structure of Ca^{2+}/CaM bound to CaMBD2 of RyR1 has shown that this area forms a strong Ca^{2+}/C-lobe binding site. However, the Ca^{2+}/N-lobe is only loosely associated and is likely to bind elsewhere.[38] We confirm these observations using ITC as the Ca^{2+}/C-lobe binds significantly stronger than the Ca^{2+}/N-lobe, with the latter affinity decreasing even further once the Ca^{2+}/C-lobe is already bound. Therefore, it is possible that the Ca^{2+}/N-lobe is associated with a different segment. Here we also analyzed the binding of apoCaM and Ca^{2+}/CaM to the two remaining candidates, which we named CaMBD1 (corresponding to RyR1 residues 1975−1999) and CaMBD3 (RyR1 residues 4295−4325).

CaMBD1 was first identified as a potential apoCaM binding site in RyR1.[35] However, using our ITC experiments, we could

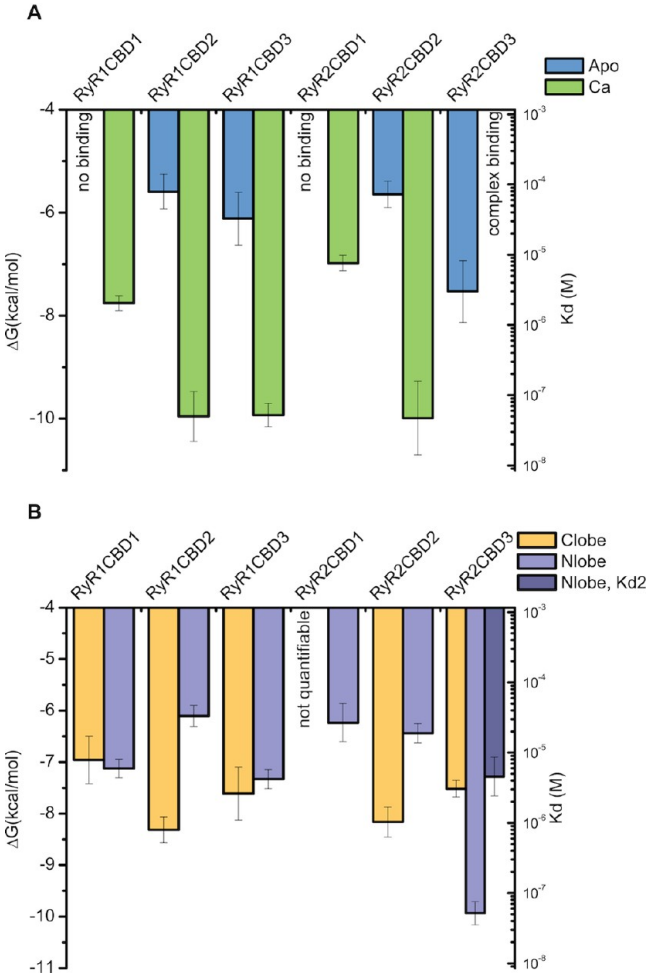

Figure 7. Overview of binding of Ca^{2+}/CaM and apoCaM to CaMBDs. Bar graphs comparing the K_d and ΔG values of binding for CaM (A) and the individual Ca^{2+}/lobes (B) to the three CaMBDs. Error bars are standard deviations.

not detect any binding of apoCaM to CaMBD1 for either RyR1 or RyR2. Instead, CaMBD1 forms only an alternative Ca^{2+}/CaM binding site, with a higher affinity for the Ca^{2+}/N-lobe than for the Ca^{2+}/C-lobe. This is especially true in RyR2, where binding of the Ca^{2+}/C-lobe to CaMBD1 individually could not be detected. A simple interpretation would then be that Ca^{2+}/CaM could bridge CaMBD1 and CaMBD2 via its N-lobe and C-lobe, respectively.

However, CaMBD3, a poorly conserved segment in the C-terminal fifth of the channel, forms an additional binding site for both Ca^{2+}/CaM and apoCaM. In fact, it forms the highest-affinity binding site we detected for CaM in the absence of Ca^{2+}, suggesting that it may form the primary apoCaM binding site. In both RyR1 and RyR2, CaMBD3 strongly bound apoCaM and is mainly mediated by the apo-N-lobe. Ca^{2+}/CaM binding is almost as strong as for CaMBD2, but the energetic profile differs substantially between RyR1 and RyR2, with even two binding sites existing for the Ca^{2+}/N-lobe in RyR1.

We also investigated physiological mutations in RyR1 CaMBD3 that have been linked to CCD, to mmCD (R4235D), and to increased creatine kinase levels/MH (LRR duplication). Neither mutation abolishes CaM binding, but both affect the energetics and likely also the binding mode, suggesting that interfering with CaM regulation at this site may be the primary cause of the disease for these specific mutations.

A crucial question is whether the CaMBDs described here also bind CaM when they are present in the native context of a full-length channel. In the absence of a high-resolution structure of the full-length protein, this is a difficult question to answer. CaM binds to RyR subunits with a 1:1 stoichiometry, which would seem to be at odds with the presence of three sites that can all bind Ca^{2+}/CaM. Two sites could bind Ca^{2+}/CaM simultaneously through the ability of individual CaM lobes to bind targets separately, a feature that has been observed in several CaM–ion channel complexes.[47,48] In addition, the sites could also be mutually exclusive, whereby binding to one site occludes the other through direct steric hindrance or allosterically. This allows redundancy in CaM binding, without affecting the 1:1 stoichiometry. Cryo-EM studies have shown that the center of mass of CaM undergoes an ∼30 Å shift on RyR1. Because CaMBD2 is able to bind both apoCaM and Ca^{2+}/CaM, it has been suggested that CaM shifts along this helix upon binding Ca^{2+}.[31,61,62] However, mere shifts within the CaMBD2 are unlikely to create the large movements observed in the cryo-EM studies. Instead, it is more likely that either one or both lobes of CaM shift to another CaMBD upon associating with Ca^{2+}. Förster resonance energy transfer (FRET) measurements between CaM and FKBP on RyRs, however, do not reveal a large shift in apoCaM and Ca^{2+}/CaM.[63] To reconcile these differences, it has been proposed that CaM moves in an arc with a constant radius relative to the donor FKBP in the FRET measurements.

The concentration of free CaM in the cytosol of cardiac myocytes has been measured to be ∼50–75 nM.[64] In addition, the affinity of CaM for intact RyR2 near cardiac myocyte Z-lines has been found to have a K_d of ∼10–20 nM,[65] comparable to the K_d values obtained by measuring binding of [^{35}S]CaM to RyRs in SR vesicles (∼20–30 nM), even at Ca^{2+} concentrations below 0.01 μM.[66] One could therefore question the relevance of individual CaMBDs with K_d values of >1 μM. However, functional studies with voltage-gated calcium channels have shown that CaM concentrations in the immediate vicinity of some targets can be enriched several orders of magnitude.[67] More importantly, because of the inherent ability of the CaM lobes to bind segments individually, it is likely that higher-affinity sites are formed by allowing the lobes to bridge noncontiguous CaMBDs, capitalizing on additive affinities. This would be most important for apoCaM, because the highest affinity we observed is ∼5 μM for RyR2 CaMBD3. Because CaMBD1 does not bind apoCaM in our experiments, an attractive possibility is thus that apoCaM bridges CaMBD2 and CaMBD3.

Importantly, for the CaMBDs to be "true" CaM binding sites, they also have to be solvent accessible within full-length RyR. Cryo-EM reconstructions using GFP insertions in full-length RyR2 localized CaMBD3 to the cytosolic surface, near the side of domain 3 and close to the cleft formed by domains 7 and 8a.[37] This is in the proximity of the Ca^{2+}/CaM binding site of RyR1 and the apoCaM site in RyR2.[40] Importantly, the GFP insertion did not create any visible conformational changes, suggesting that the site could be solvent-exposed. Similarly, GFP insertion studies show that CaMBD2 is located near domains 3 and 8a, again close to both apoCaM and Ca^{2+}/CaM sites of RyR1, and to the apoCaM site of RyR2.[37] On the other hand, two GFP insertions near CaMBD1, at positions T1874 and T2023 of RyR2, localized to domains 9 and 4, respectively.[68,69] These were interpreted to be too far from the identified CaM binding sites in

dx.doi.org/10.1021/bi401502x | *Biochemistry* 2014, 53, 932–946

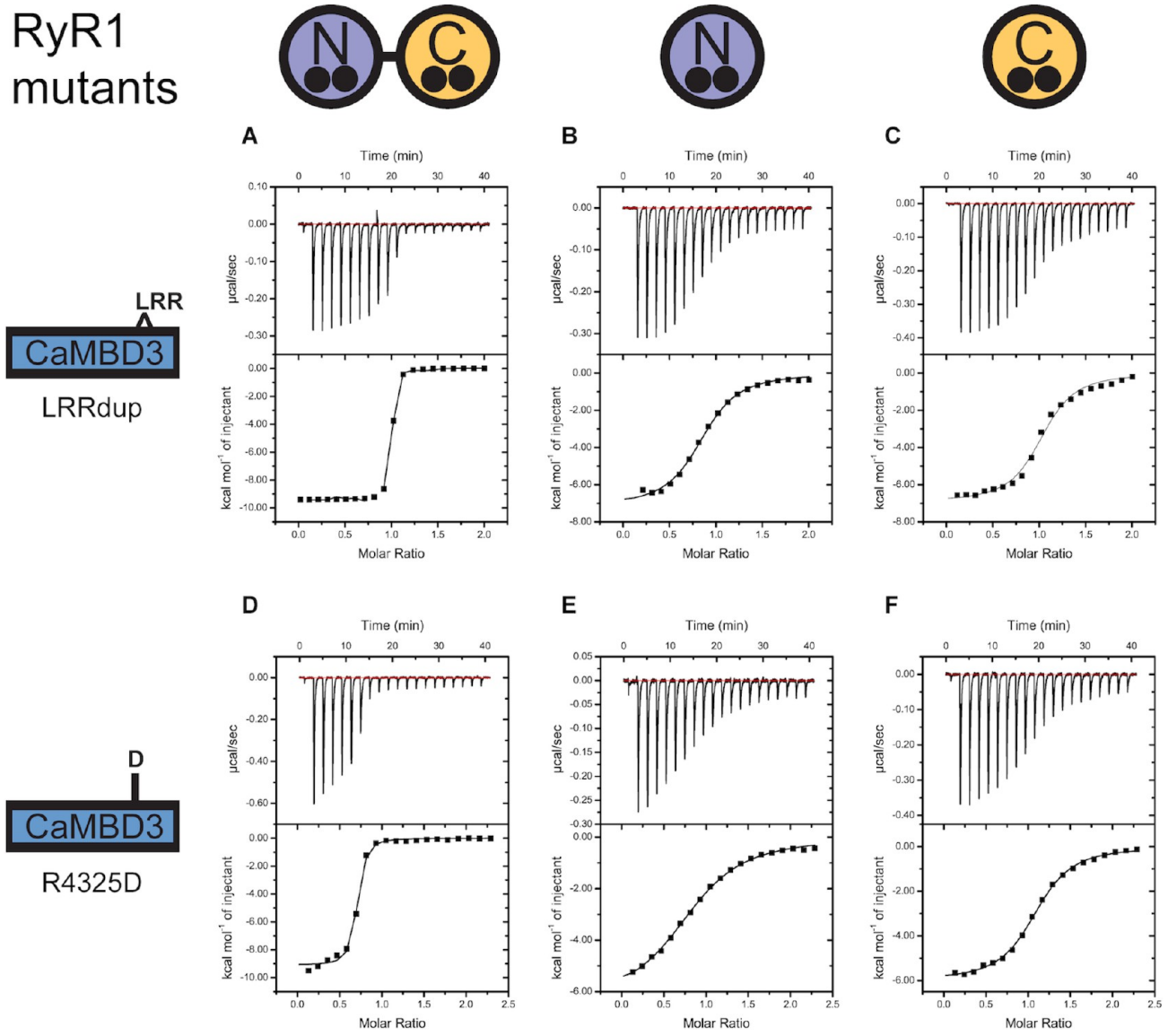

Figure 8. R4325D and LRR duplication mutants in RyR1 CaMBD3. (A–F) ITC binding isotherms show the interaction between CaM or its lobes titrated with the CaMBD3 mutants in the presence of 10 mM $CaCl_2$. The columns indicate the titrant; the rows show the CaMBD in the cell. Solid lines represent the fits. The following concentrations were used (titrant into cell): (A) 200 μM in 20 μM, (B) 400 μM in 40 μM, (C) 400 μM in 40 μM, (D) 400 μM in 35 μM, (E) 400 μM in 35 μM, and (F) 400 μM in 35 μM. Affinity and thermodynamic parameters are listed in Table 3.

cryo-EM studies. Although this would argue against the involvement of CaMBD1 in CaM binding, no insertion was conducted directly within the CaMBD1 sequence (residues 1941–1965 in RyR2), and the longer linker length used for inserting GFP (nine residues on either side of the insertion) may have created difference densities farther from the insertion site. Importantly, the insertions in CaMBD2 and CaMBD3 had used shorter linkers, so the locations of these sites are more reliable.

In addition to cryo-EM studies, the functional effect of CaM on full-length RyRs has been analyzed on a series of chimeras, deletion mutants, and point mutations. Introduction of mutations into RyR2 CaMBD2 has been shown to cause early cardiac hypertrophy in mice and in neonatal cardiomyocytes, as well as an impaired inhibition by CaM.[70] This study highlights a clear role for CaMBD2 in mediating CaM regulation.

For CaMBD1, no deletion or CaM binding knockout mutations have been generated, so a direct test of this segment in modulation by CaM has not been performed. The CaMBD1 sequences of RyR1 and RyR2 differ in 10 positions, but swapping these did not have an effect on the channel open probability at either high or low Ca^{2+} concentrations.[71] The difference in modulation of RyR1 and RyR2 by apoCaM is therefore unlikely to be due to any sequence differences in CaMBD1, but this does not preclude a role for CaMBD1 in the binding and modulation by CaM.

No deletion has been made for CaMBD3 individually, but deletion experiments have been performed on a much larger area (RyR1 residues 4274–4535), which encompasses CaMBD3.[62] Overlay binding assays showed that apoCaM and Ca^{2+}/CaM can still bind to this deletion mutant. Ca^{2+}/CaM inhibited and apoCaM activated this mutant with potencies similar to that of wild-type RyR1. These observations argue against the involvement of CaMBD3 in mediated CaM regulation of RyR1. However, CaMBD3 may still have a function. First, no deletion experiments have been performed on CaMBD3 in RyR2, and given the differences in both binding and functional effects of

dx.doi.org/10.1021/bi401502x | *Biochemistry* 2014, 53, 932–946

CaM in RyR1 and RyR2, it may still be directly involved in CaM regulation of RyR2. Second, as seen for other ion channels, there may be additional functions for CaM beyond regulation of the open probability, such as mediating proper folding and trafficking, and these may involve CaMBD3. CaM may also be able to further affect P_o in the presence of additional RyR post-translational modifications or auxiliary proteins, and this may be dependent on particular CaMBDs.

Finally, one should also consider the possibility of an EF-hand redundancy. It is frequently observed that CaM target peptides are also able to bind other EF-hand-containing proteins. For example, the IQ domain of voltage-gated calcium channels forms a known binding site for CaM[42,44,45] but is also able to bind other members of the CaBP family,[72] and even an EF-hand-containing region of RyRs.[73] Within RyRs, CaMBD2 has also been found to associate with S100A1, a dimeric EF-hand-containing protein that is thought to compete with CaM for binding RyRs.[74,75] In addition, CaMBD2 has been found to bind the same RyR EF-hand-containing region.[73,76] Many other EF-hand-containing proteins simply have not been tested yet. It is therefore possible that one or several of the RyR CaMBDs are general EF-hand binding domains, with the exact binding depending on Ca^{2+} levels and relative availabilities of the various EF-hand-containing proteins.

■ ASSOCIATED CONTENT

Supporting Information

Additional figures showing competition experiments and mutants. This material is available free of charge via the Internet at http://pubs.acs.org.

■ AUTHOR INFORMATION

Corresponding Author

*Department of Biochemistry and Molecular Biology, Life Sciences Institute, University of British Columbia, 2350 Health Sciences Mall, Vancouver, BC V6T 1Z3, Canada. E-mail: filip.vanpetegem@gmail.com. Telephone: (604) 827-4267.

Funding

Funding was provided by Canadian Institute for Health Research Grants 125893 and 259009 to F.V.P.

Notes

The authors declare no competing financial interest.

■ ACKNOWLEDGMENTS

We thank Lynn Kimlicka for maintaining a database of RyR mutations.

■ ABBREVIATIONS

apoCaM, apocalmodulin; C-lobe, C-terminal lobe of calmodulin; Ca^{2+}/CaM, Ca^{2+}-loaded calmodulin; CaM, calmodulin; CaMBD, calmodulin binding domain; CCD, central core disease; CPVT, catecholaminergic polymorphic ventricular tachycardia; CV, column volume; ER/SR, endoplasmic/sarcoplasmic reticulum; GFP, green fluoresecent protein; ITC, isothermal titration calorimetry; MH, malignant hyperthermia; N-lobe, N-terminal lobe of calmodulin; NMR, nuclear magnetic resonance; RyR, ryanodine receptor; SOICR, store overload-induced calcium release; TEV, tobacco etch virus.

■ REFERENCES

(1) Van Petegem, F. (2012) Ryanodine Receptors: Structure and Function. *J. Biol. Chem. 287*, 31624−31632.

(2) Takeshima, H., Nishimura, S., Matsumoto, T., Ishida, H., Kangawa, K., Minamino, N., Matsuo, H., Ueda, M., Hanaoka, M., Hirose, T., et al. (1989) Primary structure and expression from complementary DNA of skeletal muscle ryanodine receptor. *Nature 339*, 439−445.

(3) Otsu, K., Willard, H. F., Khanna, V. K., Zorzato, F., Green, N. M., and MacLennan, D. H. (1990) Molecular cloning of cDNA encoding the Ca^{2+} release channel (ryanodine receptor) of rabbit cardiac muscle sarcoplasmic reticulum. *J. Biol. Chem. 265*, 13472−13483.

(4) Hakamata, Y., Nakai, J., Takeshima, H., and Imoto, K. (1992) Primary structure and distribution of a novel ryanodine receptor/calcium release channel from rabbit brain. *FEBS Lett. 312*, 229−235.

(5) Endo, M., Tanaka, M., and Ogawa, Y. (1970) Calcium induced release of calcium from the sarcoplasmic reticulum of skinned skeletal muscle fibres. *Nature 228*, 34−36.

(6) Fabiato, A. (1983) Calcium-induced release of calcium from the cardiac sarcoplasmic reticulum. *Am. J. Physiol. 245*, C1−C14.

(7) Meissner, G., Darling, E., and Eveleth, J. (1986) Kinetics of rapid Ca^{2+} release by sarcoplasmic reticulum. Effects of Ca^{2+}, Mg^{2+}, and adenine nucleotides. *Biochemistry 25*, 236−244.

(8) Palade, P., Mitchell, R. D., and Fleischer, S. (1983) Spontaneous calcium release from sarcoplasmic reticulum. General description and effects of calcium. *J. Biol. Chem. 258*, 8098−8107.

(9) Jiang, D., Xiao, B., Yang, D., Wang, R., Choi, P., Zhang, L., Cheng, H., and Chen, S. R. (2004) RyR2 mutations linked to ventricular tachycardia and sudden death reduce the threshold for store-overload-induced Ca^{2+} release (SOICR). *Proc. Natl. Acad. Sci. U.S.A. 101*, 13062−13067.

(10) Fujii, J., Otsu, K., Zorzato, F., de Leon, S., Khanna, V. K., Weiler, J. E., O'Brien, P. J., and MacLennan, D. H. (1991) Identification of a mutation in porcine ryanodine receptor associated with malignant hyperthermia. *Science 253*, 448−451.

(11) Kausch, K., Lehmann-Horn, F., Janka, M., Wieringa, B., Grimm, T., and Muller, C. R. (1991) Evidence for linkage of the central core disease locus to the proximal long arm of human chromosome 19. *Genomics 10*, 765−769.

(12) Priori, S. G., Napolitano, C., Tiso, N., Memmi, M., Vignati, G., Bloise, R., Sorrentino, V., and Danieli, G. A. (2001) Mutations in the cardiac ryanodine receptor gene (hRyR2) underlie catecholaminergic polymorphic ventricular tachycardia. *Circulation 103*, 196−200.

(13) Lobo, P. A., and Van Petegem, F. (2009) Crystal structures of the N-terminal domains of cardiac and skeletal muscle ryanodine receptors: Insights into disease mutations. *Structure 17*, 1505−1514.

(14) Tung, C. C., Lobo, P. A., Kimlicka, L., and Van Petegem, F. (2010) The amino-terminal disease hotspot of ryanodine receptors forms a cytoplasmic vestibule. *Nature 468*, 585−588.

(15) Yuchi, Z., Lau, K., and Van Petegem, F. (2012) Disease mutations in the ryanodine receptor central region: Crystal structures of a phosphorylation hot spot domain. *Structure 20*, 1201−1211.

(16) Amador, F. J., Liu, S., Ishiyama, N., Plevin, M. J., Wilson, A., MacLennan, D. H., and Ikura, M. (2009) Crystal structure of type I ryanodine receptor amino-terminal β-trefoil domain reveals a disease-associated mutation "hot spot" loop. *Proc. Natl. Acad. Sci. U.S.A. 106*, 11040−11044.

(17) Sharma, P., Ishiyama, N., Nair, U., Li, W., Dong, A., Miyake, T., Wilson, A., Ryan, T., Maclennan, D. H., Kislinger, T., Ikura, M., Dhe-Paganon, S., and Gramolini, A. O. (2012) Structural determination of the phosphorylation domain of the ryanodine receptor. *FEBS J. 279*, 3952−3964.

(18) Kimlicka, L., Lau, K., Tung, C. C., and Van Petegem, F. (2013) Disease mutations in the ryanodine receptor N-terminal region couple to a mobile intersubunit interface. *Nat. Commun. 4*, 1506.

(19) Kimlicka, L., Tung, C. C., Carlsson, A. C., Lobo, P. A., Yuchi, Z., and Van Petegem, F. (2013) The Cardiac Ryanodine Receptor N-Terminal Region Contains an Anion Binding Site that Is Targeted by Disease Mutations. *Structure 21*, 1440−1449.

(20) Amador, F. J., Kimlicka, L., Stathopulos, P. B., Gasmi-Seabrook, G. M., Maclennan, D. H., Van Petegem, F., and Ikura, M. (2013) Type 2 Ryanodine Receptor Domain A Contains a Unique and Dynamic α-

Helix That Transitions to a β-Strand in a Mutant Linked with a Heritable Cardiomyopathy. *J. Mol. Biol. 425*, 4034−4046.
(21) Ikemoto, T., Iino, M., and Endo, M. (1995) Enhancing effect of calmodulin on Ca^{2+}-induced Ca^{2+} release in the sarcoplasmic reticulum of rabbit skeletal muscle fibres. *J. Physiol. 487* (Part3), 573−582.
(22) Tripathy, A., Xu, L., Mann, G., and Meissner, G. (1995) Calmodulin activation and inhibition of skeletal muscle Ca^{2+} release channel (ryanodine receptor). *Biophys. J. 69*, 106−119.
(23) Buratti, R., Prestipino, G., Menegazzi, P., Treves, S., and Zorzato, F. (1995) Calcium dependent activation of skeletal muscle Ca^{2+} release channel (ryanodine receptor) by calmodulin. *Biochem. Biophys. Res. Commun. 213*, 1082−1090.
(24) Fuentes, O., Valdivia, C., Vaughan, D., Coronado, R., and Valdivia, H. H. (1994) Calcium-dependent block of ryanodine receptor channel of swine skeletal muscle by direct binding of calmodulin. *Cell Calcium 15*, 305−316.
(25) Fruen, B. R., Bardy, J. M., Byrem, T. M., Strasburg, G. M., and Louis, C. F. (2000) Differential Ca^{2+} sensitivity of skeletal and cardiac muscle ryanodine receptors in the presence of calmodulin. *Am. J. Physiol. 279*, C724−C733.
(26) Tian, X., Tang, Y., Liu, Y., Wang, R., and Chen, S. R. (2013) Calmodulin Modulates the Termination Threshold for Cardiac Ryanodine Receptor Mediated Ca^{2+} Release. *Biochem. J. 455*, 367−375.
(27) Nyegaard, M., Overgaard, M. T., Sondergaard, M. T., Vranas, M., Behr, E. R., Hildebrandt, L. L., Lund, J., Hedley, P. L., Camm, A. J., Wettrell, G., Fosdal, I., Christiansen, M., and Borglum, A. D. (2012) Mutations in calmodulin cause ventricular tachycardia and sudden cardiac death. *Am. J. Hum. Genet. 91*, 703−712.
(28) Chen, S. R., and MacLennan, D. H. (1994) Identification of calmodulin-, Ca^{2+}-, and ruthenium red-binding domains in the Ca^{2+} release channel (ryanodine receptor) of rabbit skeletal muscle sarcoplasmic reticulum. *J. Biol. Chem. 269*, 22698−22704.
(29) Menegazzi, P., Larini, F., Treves, S., Guerrini, R., Quadroni, M., and Zorzato, F. (1994) Identification and characterization of three calmodulin binding sites of the skeletal muscle ryanodine receptor. *Biochemistry 33*, 9078−9084.
(30) Guerrini, R., Menegazzi, P., Anacardio, R., Marastoni, M., Tomatis, R., Zorzato, F., and Treves, S. (1995) Calmodulin binding sites of the skeletal, cardiac, and brain ryanodine receptor Ca^{2+} channels: Modulation by the catalytic subunit of cAMP-dependent protein kinase? *Biochemistry 34*, 5120−5129.
(31) Rodney, G. G., Moore, C. P., Williams, B. Y., Zhang, J. Z., Krol, J., Pedersen, S. E., and Hamilton, S. L. (2001) Calcium binding to calmodulin leads to an N-terminal shift in its binding site on the ryanodine Receptor. *J. Biol. Chem. 276*, 2069−2074.
(32) Yamaguchi, N., Xu, L., Pasek, D. A., Evans, K. E., and Meissner, G. (2003) Molecular basis of calmodulin binding to cardiac muscle Ca^{2+} release channel (ryanodine receptor). *J. Biol. Chem. 278*, 23480−23486.
(33) Balshaw, D. M., Xu, L., Yamaguchi, N., Pasek, D. A., and Meissner, G. (2001) Calmodulin binding and inhibition of cardiac muscle calcium release channel (ryanodine receptor). *J. Biol. Chem. 276*, 20144−20153.
(34) Xiong, L. W., Newman, R. A., Rodney, G. G., Thomas, O., Zhang, J. Z., Persechini, A., Shea, M. A., and Hamilton, S. L. (2002) Lobe-dependent regulation of ryanodine receptor type 1 by calmodulin. *J. Biol. Chem. 277*, 40862−40870.
(35) Zhang, H., Zhang, J. Z., Danila, C. I., and Hamilton, S. L. (2003) A noncontiguous, intersubunit binding site for calmodulin on the skeletal muscle Ca^{2+} release channel. *J. Biol. Chem. 278*, 8348−8355.
(36) Zhu, X., Ghanta, J., Walker, J. W., Allen, P. D., and Valdivia, H. H. (2004) The calmodulin binding region of the skeletal ryanodine receptor acts as a self-modulatory domain. *Cell Calcium 35*, 165−177.
(37) Huang, X., Liu, Y., Wang, R., Zhong, X., Koop, A., Chen, S. R., Wagenknecht, T., and Liu, Z. (2013) Two potential calmodulin binding sequences in the ryanodine receptor contribute to a mobile, intra-subunit calmodulin binding domain. *J. Cell Sci. 126*, 4527−4535.
(38) Maximciuc, A. A., Putkey, J. A., Shamoo, Y., and Mackenzie, K. R. (2006) Complex of calmodulin with a ryanodine receptor target reveals a novel, flexible binding mode. *Structure 14*, 1547−1556.
(39) Samso, M., and Wagenknecht, T. (2002) Apocalmodulin and Ca^{2+}-calmodulin bind to neighboring locations on the ryanodine receptor. *J. Biol. Chem. 277*, 1349−1353.
(40) Huang, X., Fruen, B., Farrington, D. T., Wagenknecht, T., and Liu, Z. (2012) Calmodulin-binding locations on the skeletal and cardiac ryanodine receptors. *J. Biol. Chem. 287*, 30328−30335.
(41) Kholod, N., and Mustelin, T. (2001) Novel vectors for co-expression of two proteins in *E. coli*. *BioTechniques 31*, 322−323 , 326−328.
(42) Van Petegem, F., Chatelain, F. C., and Minor, D. L., Jr. (2005) Insights into voltage-gated calcium channel regulation from the structure of the CaV1.2 IQ domain-Ca^{2+}/calmodulin complex. *Nat. Struct. Mol. Biol. 12*, 1108−1115.
(43) Edelhoch, H. (1967) Spectroscopic determination of tryptophan and tyrosine in proteins. *Biochemistry 6*, 1948−1954.
(44) Mori, M. X., Vander Kooi, C. W., Leahy, D. J., and Yue, D. T. (2008) Crystal structure of the CaV2 IQ domain in complex with Ca^{2+}/calmodulin: High-resolution mechanistic implications for channel regulation by Ca^{2+}. *Structure 16*, 607−620.
(45) Kim, E. Y., Rumpf, C. H., Fujiwara, Y., Cooley, E. S., Van Petegem, F., and Minor, D. L., Jr. (2008) Structures of CaV2 Ca^{2+}/CaM-IQ domain complexes reveal binding modes that underlie calcium-dependent inactivation and facilitation. *Structure 16*, 1455−1467.
(46) Ibarra, C. A., Wu, S. W., Murayama, K., Minami, N., Ichihara, Y., Kikuchi, H., Noguchi, S., Hayashi, Y. K., Ochiai, R., and Nishino, I. (2006) Malignant hypethermia in Japan: Mutation screening of the entire ryanodine receptor type 1 gene coding region by direct sequencing. *Anesthesiology 104*, 1146−1154.
(47) Van Petegem, F., Lobo, P. A., and Ahern, C. A. (2012) Seeing the Forest through the Trees: Towards a Unified View on Physiological Calcium Regulation of Voltage-Gated Sodium Channels. *Biophys. J. 103*, 2243−2251.
(48) Kovalevskaya, N. V., van de Waterbeemd, M., Bokhovchuk, F. M., Bate, N., Bindels, R. J., Hoenderop, J. G., and Vuister, G. W. (2013) Structural analysis of calmodulin binding to ion channels demonstrates the role of its plasticity in regulation. *Pfluegers Arch. 465*, 1507−1519.
(49) Saimi, Y., and Kung, C. (2002) Calmodulin as an ion channel subunit. *Annu. Rev. Physiol. 64*, 289−311.
(50) Pitt, G. S. (2007) Calmodulin and CaMKII as molecular switches for cardiac ion channels. *Cardiovasc. Res. 73*, 641−647.
(51) Wang, H. G., George, M. S., Kim, J., Wang, C., and Pitt, G. S. (2007) Ca^{2+}/calmodulin regulates trafficking of Ca(V)1.2 Ca^{2+} channels in cultured hippocampal neurons. *J. Neurosci. 27*, 9086−9093.
(52) Gomez-Posada, J. C., Aivar, P., Alberdi, A., Alaimo, A., Etxeberria, A., Fernandez-Orth, J., Zamalloa, T., Roura-Ferrer, M., Villace, P., Areso, P., Casis, O., and Villarroel, A. (2011) Kv7 channels can function without constitutive calmodulin tethering. *PLoS One 6*, e25508.
(53) Joiner, W. J., Khanna, R., Schlichter, L. C., and Kaczmarek, L. K. (2001) Calmodulin regulates assembly and trafficking of SK4/IK1 Ca^{2+}-activated K^+ channels. *J. Biol. Chem. 276*, 37980−37985.
(54) Biswas, S., Deschenes, I., Disilvestre, D., Tian, Y., Halperin, V. L., and Tomaselli, G. F. (2008) Calmodulin regulation of Nav1.4 current: Role of binding to the carboxyl terminus. *J. Gen. Physiol. 131*, 197−209.
(55) Block, B. A., Imagawa, T., Campbell, K. P., and Franzini-Armstrong, C. (1988) Structural evidence for direct interaction between the molecular components of the transverse tubule/sarcoplasmic reticulum junction in skeletal muscle. *J. Cell Biol. 107*, 2587−2600.
(56) Tanabe, T., Beam, K. G., Adams, B. A., Niidome, T., and Numa, S. (1990) Regions of the skeletal muscle dihydropyridine receptor critical for excitation-contraction coupling. *Nature 346*, 567−569.
(57) Tanabe, T., Beam, K. G., Powell, J. A., and Numa, S. (1988) Restoration of excitation-contraction coupling and slow calcium current in dysgenic muscle by dihydropyridine receptor complementary DNA. *Nature 336*, 134−139.
(58) Rios, E., and Brum, G. (1987) Involvement of dihydropyridine receptors in excitation-contraction coupling in skeletal muscle. *Nature 325*, 717−720.

(59) Samso, M., Feng, W., Pessah, I. N., and Allen, P. D. (2009) Coordinated movement of cytoplasmic and transmembrane domains of RyR1 upon gating. *PLoS Biol. 7*, e85.
(60) Kimlicka, L., and Van Petegem, F. (2011) The structural biology of ryanodine receptors. *Sci. China: Life Sci. 54*, 712−724.
(61) Moore, C. P., Rodney, G., Zhang, J. Z., Santacruz-Toloza, L., Strasburg, G., and Hamilton, S. L. (1999) Apocalmodulin and Ca^{2+} calmodulin bind to the same region on the skeletal muscle Ca^{2+} release channel. *Biochemistry 38*, 8532−8537.
(62) Yamaguchi, N., Xin, C., and Meissner, G. (2001) Identification of apocalmodulin and Ca^{2+}-calmodulin regulatory domain in skeletal muscle Ca^{2+} release channel, ryanodine receptor. *J. Biol. Chem. 276*, 22579−22585.
(63) Cornea, R. L., Nitu, F., Gruber, S., Kohler, K., Satzer, M., Thomas, D. D., and Fruen, B. R. (2009) FRET-based mapping of calmodulin bound to the RyR1 Ca^{2+} release channel. *Proc. Natl. Acad. Sci. U.S.A. 106*, 6128−6133.
(64) Wu, X., and Bers, D. M. (2007) Free and bound intracellular calmodulin measurements in cardiac myocytes. *Cell Calcium 41*, 353−364.
(65) Yang, Y., Guo, T., Oda, T., Chakraborty, A., Chen, L., Uchinoumi, H., Knowlton, A. A., Fruen, B. R., Cornea, R. L., Meissner, G., and Bers, D. M. (2014) Cardiac Myocyte Z-line Calmodulin is Mainly RyR2-Bound and Reduction is Arrhythmogenic and Occurs in Heart Failure. *Circ. Res. 114*, 295−306.
(66) Meissner, G., Pasek, D. A., Yamaguchi, N., Ramachandran, S., Dokholyan, N. V., and Tripathy, A. (2009) Thermodynamics of calmodulin binding to cardiac and skeletal muscle ryanodine receptor ion channels. *Proteins 74*, 207−211.
(67) Mori, M. X., Erickson, M. G., and Yue, D. T. (2004) Functional stoichiometry and local enrichment of calmodulin interacting with Ca^{2+} channels. *Science 304*, 432−435.
(68) Zhang, J., Liu, Z., Masumiya, H., Wang, R., Jiang, D., Li, F., Wagenknecht, T., and Chen, S. R. (2003) Three-dimensional localization of divergent region 3 of the ryanodine receptor to the clamp-shaped structures adjacent to the FKBP binding sites. *J. Biol. Chem. 278*, 14211−14218.
(69) Jones, P. P., Meng, X., Xiao, B., Cai, S., Bolstad, J., Wagenknecht, T., Liu, Z., and Chen, S. R. (2008) Localization of PKA phosphorylation site, Ser(2030), in the three-dimensional structure of cardiac ryanodine receptor. *Biochem. J. 410*, 261−270.
(70) Yamaguchi, N., Takahashi, N., Xu, L., Smithies, O., and Meissner, G. (2007) Early cardiac hypertrophy in mice with impaired calmodulin regulation of cardiac muscle Ca release channel. *J. Clin. Invest. 117*, 1344−1353.
(71) Yamaguchi, N., Xu, L., Evans, K. E., Pasek, D. A., and Meissner, G. (2004) Different regions in skeletal and cardiac muscle ryanodine receptors are involved in transducing the functional effects of calmodulin. *J. Biol. Chem. 279*, 36433−36439.
(72) Findeisen, F., and Minor, D. L., Jr. (2010) Structural basis for the differential effects of CaBP1 and calmodulin on Ca(V)1.2 calcium-dependent inactivation. *Structure 18*, 1617−1631.
(73) Xiong, L., Zhang, J. Z., He, R., and Hamilton, S. L. (2006) A Ca^{2+}-binding domain in RyR1 that interacts with the calmodulin binding site and modulates channel activity. *Biophys. J. 90*, 173−182.
(74) Wright, N. T., Prosser, B. L., Varney, K. M., Zimmer, D. B., Schneider, M. F., and Weber, D. J. (2008) S100A1 and calmodulin compete for the same binding site on ryanodine receptor. *J. Biol. Chem. 283*, 26676−26683.
(75) Prosser, B. L., Wright, N. T., Hernandez-Ochoa, E. O., Varney, K. M., Liu, Y., Olojo, R. O., Zimmer, D. B., Weber, D. J., and Schneider, M. F. (2008) S100A1 binds to the calmodulin-binding site of ryanodine receptor and modulates skeletal muscle excitation-contraction coupling. *J. Biol. Chem. 283*, 5046−5057.
(76) Gangopadhyay, J. P., and Ikemoto, N. (2008) Interaction of the Lys(3614)-Asn(3643) calmodulin-binding domain with the Cys(4114)-Asn(4142) region of the type 1 ryanodine receptor is involved in the mechanism of Ca^{2+}/agonist-induced channel activation. *Biochem. J. 411*, 415−423.